



Journal homepage: anau.am/scientific-journal

doi: [10.52276/25792822-2023.2-117](https://doi.org/10.52276/25792822-2023.2-117)

UDC 631.317

Development and Justification of a Self-Regulating System for Adjusting the Angle of Rotary Tiller Blade with a Vertical Rotation Axis

A.P. Tarverdyan, A.V. Altunyan, A.S. Grigoryan

Armenian National Agrarian University

arshaluystar@gmail.com, artur_altunyan@mail.ru, algrig1968@mail.ru

ARTICLE INFO

Keywords:

*tiller,
blade installation angle,
cutting angle change,
resistance moment
equilibrium,
adjustment of installation
angle*

ABSTRACT

The article considers the problem of providing constant or almost constant values of the blade cutting angles during one rotation of the tiller rotor with a vertical rotation axis. Analytical expressions were obtained by analyzing the trajectory of the tiller knife/blade, which enable to determine the change of the blade cutting angles at a constant location and to define the patterns of this change in the ranges of $(0...π)$ and $(π...2π)$.

The derived expressions and conclusions make it possible to adjust the location angle of the knife, using a pattern, in case of which the cutting angles of the knife will remain unchanged during one rotation of the rotor. This circumstance is important from the prospect of ensuring a uniform working mode of the rotary tiller.

Introduction

Row-spacing activities are of key importance in terms of labor-intensive priority action among the overall agrotechnical measures implemented in the orchards and vineyards (Damanauskas, et al., 2019; Acharya, et al., 2019; Schjønning & Rasmussen, 2000). The latter accounts for the activation of plants and soils biological processes, an efficient fight against weeds and pests, and finally for the yield capacity and product quality (Monoenkov, 2017).

The mentioned activities are possible to carry out with increased quality and in compliance with the times set

per agrotechnical conditions only through their complete mechanization process.

The operational practice of rotary tillers in orchards has indicated that machines with active working parts are more efficient (Monoenkov, 2017; Tarverdyan, et al., 2022; Tarverdyan, et al., 2023; Panov and Tokushev, 2005; Koval, 2010; Kupryashkin and Gusev, 2020).

The first rotary tillers with active working parts were designed in the middle of the 19th century. In 1850 the Englishman Hoskins published a scientific paper, where he proposed to cultivate the soil with rotary tools similar to a tiller.

The question under discussion aims to provide the most constant values of the blade cutting angles during one rotation of the tiller, since only then the equilibrium in the changes of moment loads generated from the factors of resistance forces applied to the rotor shaft can be provided. It is obvious that in this case the blade installation angle γ has to be changed or adjusted.

Usually, in case of similar problems, such a constant angle for the blade installation is identified, in which case the front and back cutting angles of the blade arm will receive optimal values from the point of view of the energy efficiency of the technological process during one rotation of the rotor. Based on the goal of the problem, let's try to solve the "inverse" problem and, based on the results, develop an adjustment system for the blade installation angle.

Since the installation and cutting angles of the blade arm are related to the angle ($\Delta\varepsilon$) formed by the tangents to the cycloidal and circle of radius R at the given point of the trajectory, it is obvious that first the angles formed by the said tangents to the positive direction of x and patterns of their change during one rotation of the rotor should be determined.

Observing the movement of any point of the blade in a circle with radius R, we can write:

$$\left. \begin{aligned} x &= R \sin \omega t, \\ y &= R \cos \omega t. \end{aligned} \right\} \quad (3)$$

Projections of the moving speeds of the point will be:

$$\left. \begin{aligned} V_x &= \frac{dx}{dt} = R\omega \cdot \cos \omega t \\ V_y &= \frac{dy}{dt} = -R\omega \cdot \sin \omega t \end{aligned} \right\} \quad (4)$$

The angle formed by the tangent at any point on the circle will be determined as follows:

$$\operatorname{tg} \theta_2 = \frac{dy}{dx} = -\frac{\sin \omega t}{\cos \omega t} = -\operatorname{tg} \varphi. \quad (5)$$

The equation of a point movement with a real trajectory – a cycloid – is described by the expression (1), the components of the velocity will then be:

$$\left. \begin{aligned} V_x &= \frac{dx}{dt} = V_p \pm R\omega \cdot \cos \omega t \\ V_y &= \frac{dy}{dt} = -R\omega \sin \omega t \end{aligned} \right\} \quad (6)$$

The equation of the tangent extended at any point of the cycloid will look like this:

$$\operatorname{tg} \theta_1 = \frac{dy}{dx} = -\frac{R\omega \sin \omega t}{V_p \pm R\omega \cos \omega t}, \quad (7)$$

or $\theta_1 = -\operatorname{arctg} \left(\frac{\lambda \sin \varphi}{1 \pm \lambda \cos \varphi} \right)$, where $\lambda = \frac{R\omega}{V_p}$ is the kinematic parameter of the rotary tiller.

From (5) $\theta_2 = -\varphi$ hence the angle formed by the two tangents extended at the arbitrary A point of the trajectory – $\Delta\varepsilon_4$ – will be (Figure 1):

$$\Delta\varepsilon_4 = \theta_1 - \theta_2 = -\operatorname{arctg} \left(\frac{\lambda \sin \varphi}{1 \pm \lambda \cos \varphi} \right) + \varphi. \quad (8)$$

From the point of view of the relevancy of further analysis, the following can be determined from ΔAPK (Figure 1):

$$V_p^2 = V_0^2 + V_A^2 - 2V_0V_A \cos \Delta\varepsilon, \quad (9)$$

where $V_0 = \omega R$ is the circumferential velocity of point A, V_A is the total velocity of A point, directed by the tangent to the cycloid at that point, the module of which is determined through the following expression:

$$V_A = \sqrt{V_x^2 + V_y^2}, \text{ or placing from (6) –}$$

$$V_A = \sqrt{V_p^2 + V_0^2 \pm 2V_pV_0 \cdot \cos \varphi}. \text{ Placing in (9) we'll get:}$$

$$\cos \Delta\varepsilon = \frac{V_0^2 \pm V_pV_0 \cdot \cos \varphi}{V_0 \sqrt{V_p^2 + V_0^2 \pm 2V_pV_0 \cdot \cos \varphi}} \text{ or,}$$

$$\Delta\varepsilon = \operatorname{arc} \cos \left(\frac{\lambda \pm \cos \varphi}{\sqrt{1 + \lambda^2 \pm 2\lambda \cdot \cos \varphi}} \right). \quad (10)$$

Deriving (10) expression per and equating to 0 we'll have:

$$\Delta\varepsilon' = -\frac{1}{\sqrt{1 - \frac{\lambda \pm \cos \varphi}{\sqrt{1 + \lambda^2 \pm 2\lambda \cos \varphi}}}} \cdot \left(\frac{\lambda \pm \cos \varphi}{\sqrt{1 + \lambda^2 \pm 2\lambda \cos \varphi}} \right) = 0,$$

$$\text{or } 2(1 + \lambda^2) \sin \varphi \mp 4\lambda \cos \varphi \cdot \sin \varphi - 2\lambda^2 \sin \varphi \pm 2\lambda \sin \varphi \cdot \cos \varphi = 0$$

$$\sin \varphi (1 \pm \lambda \cos \varphi) = 0. \quad (11)$$

It follows from the expression (11), when $\varphi = \{0; \pi; 2\pi\}$, $\Delta\varepsilon = \Delta\varepsilon_{\min} = 0$ and when $\varphi_1 = \operatorname{arccos} \left(\mp \frac{1}{\lambda} \right)$ and $\varphi_2 = \varphi_1 + \pi$, $\Delta\varepsilon$ acquires the maximum value:

$$\Delta\varepsilon = \Delta\varepsilon_{\max} = \operatorname{arccos} \frac{\lambda^2 - 1}{\lambda \sqrt{\lambda^2 - 1}}. \quad (12)$$

Since during one rotation of the rotor $\Delta\varepsilon$ changes the sign $\Delta\varepsilon = \theta_1 - \theta_2$ (Figure 1), in the range of $0 \leq \varphi \leq \pi$ $\theta_1 > \theta_2$, and in that of $\pi \leq \varphi \leq 2\pi$ $\theta_1 < \theta_2$, hence the changing pattern of $\Delta\varepsilon$ should be discussed in two variants:

$$\Delta\varepsilon = \pm \operatorname{arccos} \frac{\lambda \pm \cos \varphi}{\sqrt{1 + \lambda^2 \pm 2\lambda \cos \varphi}}, \quad (13)$$

The variant with "+" has been analysed, while in case of "-" sign, when $\varphi = \{0; \pi; 2\pi\}$, we'll have:

$$\Delta\varepsilon = \Delta\varepsilon_{\max} = 0 \text{ and when } \varphi_1 = \operatorname{arccos} \left(\mp \frac{1}{\lambda} \right) \text{ and } \varphi_2 = \varphi_1 + \pi$$

$$\Delta\varepsilon = \Delta\varepsilon_{\min} = -\arccos \frac{\lambda^2 - 1}{\lambda\sqrt{\lambda^2 - 1}} \text{ (obviously } \lambda \geq 1) \quad (14)$$

$\Delta\varepsilon = \pm f(\varphi)$ (diagrams are introduced in Figure 2).

Results and discussions

Based on the theoretical and practical research results related to the rotary machines with vertical rotation axis (Tarverdyan, et al., 2022, Tarverdyan, et al., 2023, Tarverdyan and Sargsyan, 2015), during the design of diagrams we have found it relevant to take the following geometrical and kinematical values as baseline data: $R=0.35 \text{ m}$; $\omega=11 \text{ s}^{-1}$; $\lambda=3.85$; $V_p=1.0 \text{ m/s}$.

The diagrams show (Figure 2), that the signs of the members in (13) expression ($\pm 2\lambda \cos\varphi$) do not affect the modules of $\Delta\varepsilon_{\max}$ and $\Delta\varepsilon_{\min}$; only their values are derived from different values.

Thus, in case of “+” sign of the mentioned members, when the expression is also with “+” sign: $\Delta\varepsilon_{\min}=0$, when $\varphi=\{0; \pi; 2\pi\}$; $\Delta\varepsilon_{\max}=15^\circ$ when $\varphi \approx \{105^\circ \text{ and } 255^\circ\}$; (ABCDE curve in Figure 2).

In case of “-” sign of the expression (AMCNE curve in Figure 2a) $\Delta\varepsilon_{\max}=0$, when $\varphi=\{0; \pi; 2\pi\}$ and $\Delta\varepsilon_{\min}=-15^\circ$, when $\varphi \approx \{105^\circ \text{ and } 255^\circ\}$.

In case of the sign “-” of $\cos\varphi$ and $2\lambda \cos\varphi$ members when the expression is with “+” sign: $\Delta\varepsilon_{\min}=0$, when $\varphi=\{0; \pi; 2\pi\}$ and $\Delta\varepsilon_{\max}=15^\circ$, when $\varphi \approx \{75^\circ \text{ and } 285^\circ\}$ (ABCDE curve in Figure 2b), in case of “-” sign of the expression: $\Delta\varepsilon_{\max}=0$, when $\varphi=\{0; \pi; 2\pi\}$ and $\Delta\varepsilon_{\min}=15^\circ$, and $\varphi \approx \{75^\circ \text{ and } 285^\circ\}$ (AMCNE curve in Figure 2 b).

The real change of the cutting angle in the tiller’s blade during one rotation of the rotor ($\Delta\varepsilon$) is described in the range of $0 \leq \varphi \leq \pi$ with ABC curve, whereas in $\pi \leq \varphi \leq 2\pi$ range - with CNE curve or in the range of $\pi \leq \varphi \leq \pi$ - with AMC curve, while in $\pi \leq \varphi \leq 2\pi$ range - with CDE curve (Figure 2), depending on the direction of rotor’s rotation. This statement is of vital significance in view of the objective of the problem discussed.

The changing pattern of the cutting angle in the rotor’s blade depending on the kinematic parameters of the unit gives a ground to induce important judgements from the practical perspectives: the uniformity of the work in the rotary tiller with vertical rotation axis can be ensured, particularly in case of relatively high values of kinematic parameters, but their structural features and the requirements for the implemented technological processes do not allow the kinematic parameters to be increased beyond the size determined for practical considerations. Therefore, the only way to solve the problem is to adjust the blade location during the work.

The relationships between the blade location, cutting angles and their changes have the following form:

$$\gamma = \frac{\pi}{2} - \beta + i - \Delta\varepsilon \quad (15)$$

This relationship is well-known and has been always discussed from one perspective: γ and ψ are constants; the changing parameters of β and $\Delta\varepsilon$ during single rotation of the rotor in case of different values of γ and i have been studied (Panov and Tokushev, 2005; Kupryashkin and Gusev, 2020; Chatkin, 2008).

In the current case the changing parameter of γ is considered, in case of which the cutting angle β keeps the optimal constant or almost constant value during single rotation.

Placing $\Delta\varepsilon$ value in (15), we’ll get the following from (13):

$$\gamma(\varphi) = \frac{\pi}{2} - \beta + i \mp \arccos \left(\frac{\lambda \pm \cos\varphi}{\sqrt{1 + \lambda^2 \pm 2\lambda \cos\varphi}} \right)$$

i is the sharpening angle of the blade, it is constant in each specific problem, we assume that β is also constant as a precondition and hence assigning $\frac{\pi}{2} - \beta + i = K$ we can write:

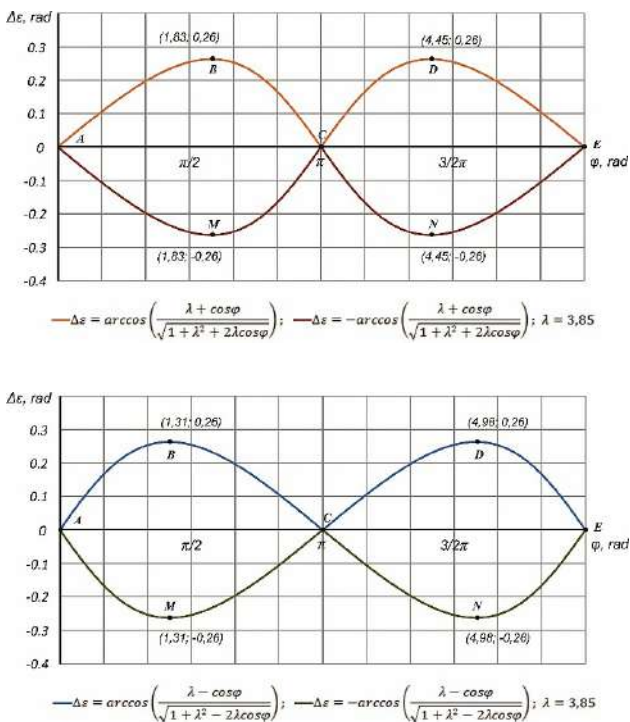


Figure 2. Diagrams of $\Delta\varepsilon = \pm f(\varphi)$ function throughout single rotation of the tiller’s rotor ($\gamma = const$) (composed by the authors).

$$\gamma(\varphi) = K \mp \arccos\left(\frac{\lambda \pm \cos \varphi}{\sqrt{1 + \lambda^2 \pm 2\lambda \cos \varphi}}\right). \quad (16)$$

The extreme points of $\gamma=f(\varphi)$ function are determined in the same way, as in case of $\Delta\varepsilon$ investigation.

It follows from $\gamma'(\varphi)=0$ condition, that $\gamma(\varphi)_{\min}^{\max}$ points are

determined from the conditions of
$$\begin{cases} \sin \varphi = 0 \\ \cos \varphi = \mp \frac{1}{\lambda} \end{cases}$$

It is relevant to track the changing regularities of γ depending on the rotor's rotation angle (φ) by the above stated example identifying also the optimal value of K constant based on the results of theoretical and practical research conducted in the previous years (Tarverdyan, et al., 2022; Tarverdyan, et al., 2023; Panov and Tokushev, 2005; Kupryashkin and Gusev, 2020; Chatkin, 2008).

Let's assume that $\beta=28^\circ$; $i=20^\circ$, in case of those values $K=1.43$ rad. The dependence graphs (diagrams) $\gamma=f(\varphi)$ have been designed for the same variants and cases, as in the case of $\Delta\varepsilon=f(\varphi)$ diagrams.

The value of blade installation angle (γ) in case of $\varphi=\{0;\pi; 2\pi\}$ values $\gamma_0=K=1.43$ rad., in (16) expression in case of "+" sign in $\cos\varphi$ and $2\lambda\cos\varphi$, $\gamma_{\max}=1.693$ rad ($\approx 97^\circ$), $\gamma_{\min}=1.1697$ rad ($66^\circ 52'$), when respectively $\varphi=\{1.834$ rad $\approx (105^\circ)$ and 4.45 rad $\approx (255^\circ)\}$.

In case of "-" sign: the values of γ_{\max} and γ_{\min} are the same as in the previous case.

In all cases in the considered example $\Delta\gamma=\pm 0,263$ rad, which is equal to $\pm\Delta\varepsilon$.

The results indicate that upon the regulation of the installation angle (γ) of the tiller's blade, it is quite possible to ensure a constant value for the blade cutting angle during a single rotation of the rotor. It should be taken into consideration that if the selected rotation direction of the rotor is in the way that $\Delta\varepsilon=f(\varphi)$ dependence is described with $A'B'C'N'E$ curve (Figure 2), then the regulation of γ should be implemented through curve (Figure 3), considering the manifestation of the functions in the ranges of $0\leq\varphi\leq\pi$ and $0\leq\varphi\leq 2\pi$, depending on the signs of $\cos\varphi$ and $2\lambda\cos\varphi$ members.

In case of self-regulating blade of the rotary tiller it is necessary to ensure the $\gamma_{\min} = \frac{\pi}{2} - \Delta\varepsilon_{\max}$ condition for the effective soil treatment (Panov and Tokushev, 2005), upon $\gamma_{\min} > \Delta\varepsilon_{\max}$. Assuming that in the boundary case $\gamma_{\min} = \Delta\varepsilon_{\max}$, considering (14) expression and modifying (16) expression, we can get:

$$K \pm \arccos\left(\frac{\sqrt{\lambda^2 - 1}}{\lambda}\right) = \pm \arccos\left(\frac{\sqrt{\lambda^2 - 1}}{\lambda}\right), \quad (17)$$

wherefrom $K = \pm 2 \arccos \frac{\sqrt{\lambda^2 - 1}}{\lambda}$ ("-" sign doesn't have any sense, since $K > 0$) and hence from the first expression the minimum boundary value of λ will be:

$$\frac{\sqrt{\lambda^2 - 1}}{\lambda} = \cos \frac{K}{2} \text{ or } \lambda_u = \frac{1}{\sin \frac{K}{2}}. \quad (18)$$

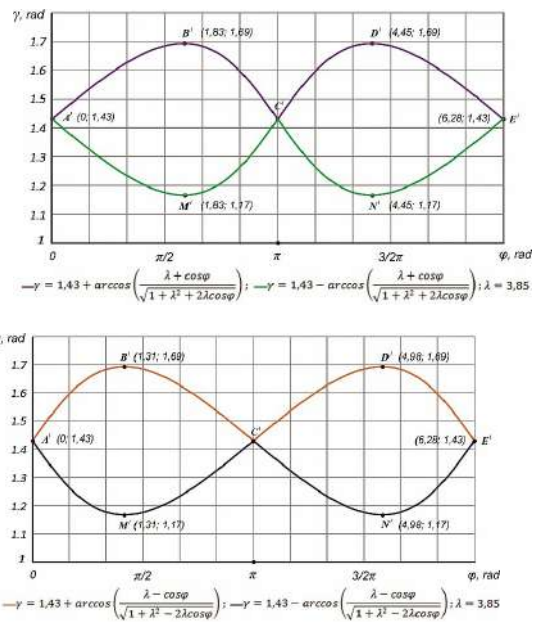


Figure 3. The diagram of $\gamma=f(\varphi)$ function during a single rotation of the rotor in case of constant cutting angles (composed by the authors).

It is obvious that for the selected K constant the real kinematical parameter (λ) of the rotary tiller should be higher than the boundary value (λ_u) of the parameter estimated via (18) expression.

Identifying and accepting the kinematical, geometrical and optimal parameters of the blade installation angles of the rotary tiller - R ; V_p ; ω ; λ ; γ ; β ; ε ; i - necessary to regulate (change) the γ according to (16) expression, so that β could stay possibly constant.

After setting up the changing function of the blade installation angle (γ), related to $\beta=const$ condition, the next important step is the implementation of γ changing pattern during a single rotation of the rotor. The regulation of the blade installation angle (γ) is possible to carry out

through different technical solutions, particularly through mechanical copying with the impact of resistance forces using inertial and elastic elements (there will be a separate reference to this issue in the near future).

In all solution options, in addition to $\gamma(\varphi)=f(\varphi)$ function, it is necessary to also have the variation graphs of velocities and accelerations for the blade arbitrary point depending on the rotation angle of the rotor (φ).

The velocity graph (Figure 4) has been designed per (6) expressions, whereas that of acceleration – per the (20) expressions presented below.

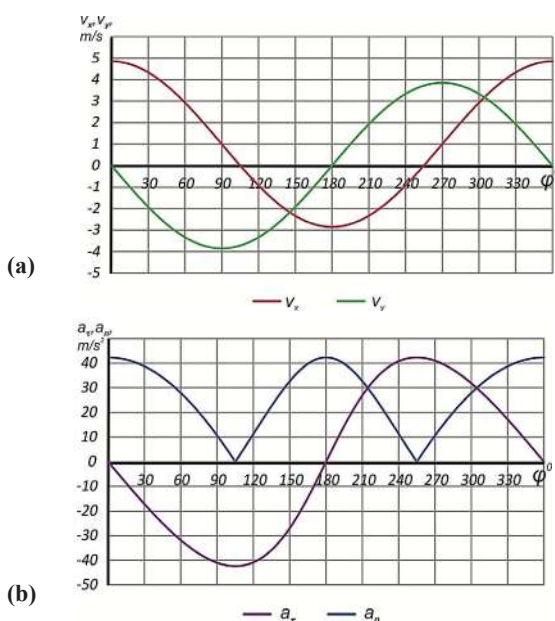


Figure 4. Variation graphs of velocity(v_x, v_y) (a) and acceleration (a_τ, a_n) (b) components of the fixed point in the rotor’s blade (composed by the authors).

Since the rotor rotates at a constant angular speed $\omega=const$, there is, therefore only centripetal acceleration $a_n(\omega)=\omega^2R$, which, however, has both normal and tangential components to the cycloid trajectory.

$$\left. \begin{aligned} a_\tau &= R\omega^2 \sin \theta_1 \\ a_n &= R\omega^2 \cos \theta_1 \end{aligned} \right\}, \quad (19)$$

where θ_1 is the angle formed by the tangent drawn to the real trajectory of the fixed point of the blade and x axis with positive direction in the case of an arbitrary rotation angle φ of the rotor. Considering that according to the (7) expression:

$\theta_1 = -arctg\left(\frac{\lambda \sin \varphi}{1 \pm \lambda \cos \varphi}\right)$, hence, the acceleration components will be:

$$\left. \begin{aligned} a_\tau &= R\omega^2 \sin \left[-arctg\left(\frac{\lambda \sin \omega t}{1 \pm \lambda \cos \omega t}\right) \right] \\ a_n &= R\omega^2 \cos \left[-arctg\left(\frac{\lambda \sin \omega t}{1 \pm \lambda \cos \omega t}\right) \right] \end{aligned} \right\}, \quad (20)$$

Another important factor in the regulation process of blade installation angle is the disclosure of variation patterns of resistance forces. Accepting that the resistance force of the blade is directed to the total velocity of the blade (V_A) along the vector’s impact line and has the opposite direction (Tarverdyan, et al., 2023; Akimov and Konstantinov, 2018; Konstantinov, 2019) we can draw out the torque value applied to the rotor’s shaft.

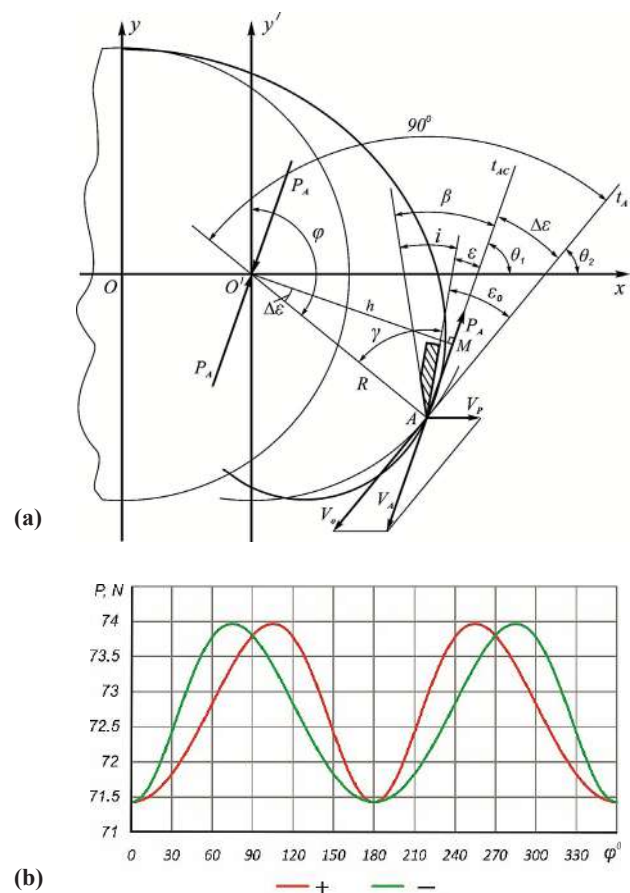


Figure 5. The diagram of determination of resistance moment applied to the tiller’s rotor shaft (5a) and the graphs of variations of resistance force applied to the tiller’s blade (5b). (composed by the authors).

$M_r = P_A \cdot h$, where $h = R \cdot \cos \Delta \epsilon$, is the arm of force couple (Figure 5a). By placing the h value, considering the (10) and accepting, that the external moment (M) applied to the rotor shaft balances the resistance moment, for P_A force we can have the following:

$$P_A = \frac{M}{R \cdot \cos \left[\arccos \left(\frac{\lambda \pm \cos \varphi}{1 + \lambda^2 \pm 2\lambda \cos \varphi} \right) \right]} = \frac{M \sqrt{1 + \lambda^2 \pm 2\lambda \cos \varphi}}{(\lambda \pm \cos \varphi) \cdot R} \quad (21)$$

Variation graphs for P_A are introduced in Figure (5b). The changing pattern of P_A during a single rotation period of the rotor should serve as a background for γ regulation with the account for the impact of resistance forces and selection of the blade's geometric form.

Conclusion

As a result of analysis of the blade trajectory in the rotary tiller with vertical rotation axis several analytical expressions have been derived, which describe the changing patterns of the blade cutting angle during a single blade rotation; besides, it has been identified that the axis perpendicular to the movement direction of the unit divides the trajectory into two domains in which the expressions for the determination of the cutting angle changes are different.

The derived expressions enable to solve the problem of keeping the cutting angles in a constant state throughout a single rotation period of the rotor by means of regulating (self-regulation) the blade's installation angle, which is of utmost significance from the prospect of ensuring uniform working mode for the rotary machine.

References

- Acharya, B.S., Dodla, S., Gaston, L.A., Darapuneni, M., Wang, J.J., Sepat, S. (2019). Winter Cover Crops Effect on Soil Moisture and Soybean Growth and Yield under Different Tillage Systems. *Soil and Tillage Research*, 104430 <https://doi.org/10.1016/j.still.2019.104430>.
- Akimov, A.P. (2013). Methodology for Calculating the Resistance and Resistance Moment to Soil Cutting / Akimov A.P., Konstantinov Yu.V., Feodorov D.I. / *Tractors and Agricultural Machines*, - № 3, - pp. 32-35.
- Akimov, A.P., Konstantinov, Yu.V. (2018). Mathematical Model of the Interaction of the Cutting Blade with the Soil. *Bulletin of Kazan State Agrarian University*, Volume 12, № 4, - pp. 29-35.
- Chatkin, M.N. (2008). Kinematics and Dynamics of Rotary Tiller Working Parts with Screw Elements. Publishing House of the Mordovian University, Saransk, - 316 p.
- Damanauskas, V., Velykis, A., and Satkus, A. (2019). Efficiency of Disc Harrow Adjustment for Stubble Tillage Quality and Fuel Consumption. *Soil & tillage Research* 194, - 104311 <https://doi.org/10.1016/j.still.2019.104311>.
- Konstantinov, Yu.V. (2019). Method for Calculating the Resistance and Resistance Moment to Soil Cutting with a Straight Lamellar Cutting Blade. *Tractors and Agricultural Machines*, Volume 86, - № 5, - pp. 31-39.
- Koval, Zh.L. (2010). Development of Rotary Tiller with Energy-Saving Cutting Working Parts. PhD for the Candidate of Technical Sciences, Moscow.
- Kupryashkin, V.F., Gusev, A.Yu. (2020). Justification of Parameters and Modes of Operation of a Self-Propelled Rotary Tiller with Combined Rotation of Active Working Parts. *Scientific Review. International Scientific and Practical Journal*, - № 2, Saransk, - pp. 42-48.
- Monoenkov, K.A. (2017). Improving Tillage in the Near-Trunk Strips of Intensive Orchards. *Technologies of the Food and Processing Industry*. Michurinsk, - № 3.
- Panov, I.M., Tokushev, Zh.E. (2005). Theory, Design and Calculation of Rotary Tillers. Publishing House of Kokshetau University, Kokshetau, - 314 p.
- Schjønning, P. & Rasmussen, K.J. (2000). Soil Strength and Soil Pore Characteristics for Direct Drilled and Ploughed Soils. *Soil and Tillage Research*, 57, 69e82 [https://doi.org/10.1016/S0167-1987\(00\)00149-5](https://doi.org/10.1016/S0167-1987(00)00149-5).
- Tarverdyan, A., Petrosyan, P., Sargsyan, S. (2015). The Kinematic of Tiller with Vertical Axis for the Cultivation of Inter-Trunk Spaces in Orchards. *Bulletin of National Agrarian University of Armenia*, - № 3, - pp. 93-99 <https://doi.org/10.1016/j.aasci.2017.03.004>.
- Tarverdyan, A., Sargsyan, S. (2015). The Dynamic of Tiller with Vertical Axis for the Cultivation of Inter-Trunk Spaces in Orchards/Bulletin of National Agrarian University of Armenia, - №4, - pp. 75-84 <https://doi.org/10.1016/j.aasci.2017.03.004>.
- Tarverdyan, A.P., Altunyan, A.V., Grigoryan, A.S. (2023). Dynamic Study of Planetary Drive Mechanism in the Orchard Rotary Tiller, "Agriscience and Technology", ANAU International Journal, № 1/81, - pp. 9-15 <https://doi.org/10.52276/25792822-2023.1-9>.
- Tarverdyan, A.P., Grigoryan, A.S., Altunyan, A.V. (2022). Kinematic Study of Orchard Rotary Tiller with a Planetary Drive. "Agriscience and Technology", ANAU International Scientific Journal, № 3/79, - pp. 231-237 <https://doi.org/10.52276/25792822-2022.3-231>.
- Vorobyov, V.A., Marchenko, O.S. (1990). Rational Arrangement of Blades on the Tiller's Drum. *Agricultural Machinery*. M., - № 2, - pp. 19-25.

Acknowledgements

The work was supported by the Science Committee of MESCS RA, in the frames of the research project № 21APP-2D015.

Accepted on 26.05.2023

Reviewed on 13.06.2023